

Supplementary Information

## Luminescent Zn-MOF for detection of explosives and development of fingerprints

Ajay Kumar<sup>a</sup>, Subhash Chandra Sahoo,<sup>a</sup> Surinder Kumar Mehta<sup>a</sup>, Parmod Soni,<sup>b</sup>  
Vishal Sharma<sup>c\*</sup> and Ramesh Kataria<sup>a\*</sup>

<sup>a</sup>Department of Chemistry, Panjab University, Chandigarh-160014, India

<sup>b</sup>Department of Chemistry, Terminal Ballistics Research Laboratory (TBRL), Defence Research and Development Organisation, Chandigarh- 160003, India

<sup>c</sup>Institute of Forensic Science & Criminology, Panjab University, Chandigarh-160014, India

E-mail: rkataria@pu.ac.in, vsharma@pu.ac.in

### Figures:

S. No.	Contents
S 1	N <sub>2</sub> adsorption-desorption study of PUC1
S 2	PXRD pattern of PUC1 before and after addition of PETN and Tetryl.
S 3	Thermogravimetric analysis curves of <b>PUC1</b> before and after treatment with PETN and Tetryl.
S 4	Fluorescence spectra of free ligand and PUC1 (inset) optical image of ligand and MOF in UV chamber.
S 5	CIE 1931 chromaticity diagram of PUC1
S 6	Fluorescence spectra of PUC1 with time up to 48 hours.
S 7	The fluorescence spectra of PUC1 before and after addition of PETN, Tetryl, TATB, TNT, HMX and RDX (50µM).
S 8	Quenching efficiency of different explosive compounds.
S9	Fluorescence spectra of PUC1 before and after the addition of different solvents.
S10-S14	Fluorescence spectra of <b>PUC1</b> by gradual addition of PETN, Tetryl, TNT, HMX and RDX.
S15-S19	Estimation of limit of detection of <b>PUC1</b> for PETN, Tetryl, TNT, HMX and RDX.
S20-S24	Stern-Volmer plots of <b>PUC1</b> by gradual addition of PETN, Tetryl, TNT, HMX and RDX.
S25	Optical images of PUC1 before and after addition of analytes under UV light
S26	FTIR spectra of <b>PUC1</b> before and after addition of PETN and Tetryl.
S27	FL spectra of Tetryl only

S28	Tauc plots of PUC1 and analytes
S29	Response time figure
S30	PXRD spectra of PUC1 at different temperatures.

**Tables:**

Table S. No.	Content
S1	Crystallographic table
S2	Bond length table for PUC1
S3	Band Gap table
S4	Comparison table for LOD.

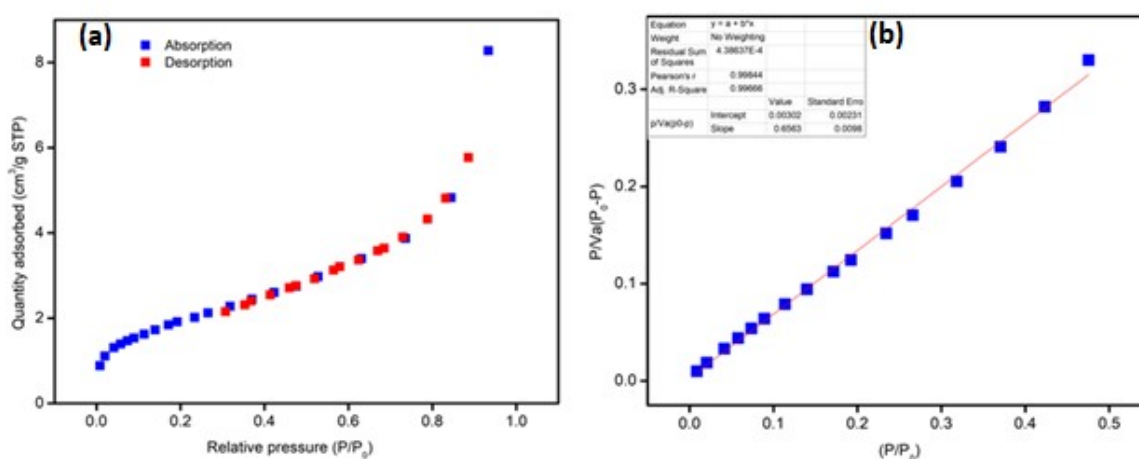


Figure S1: (a) N<sub>2</sub> adsorption (Blue) and desorption (Red) isotherms of thermally activated PUC1 measured. The samples were heated at 100°C under vacuum for 12 h before the sorption measurement. (b) BET plot.

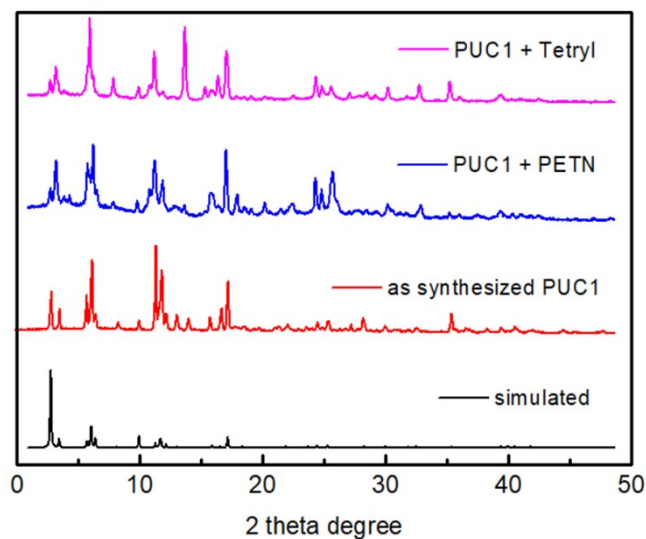


Figure S2: PXRD pattern of PUC1 before and after addition of PETN and Tetryl.

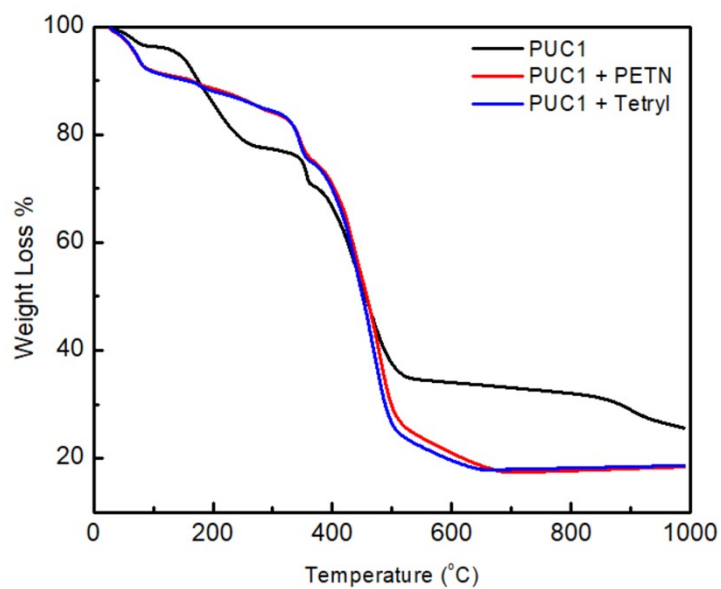


Figure S3: Thermogravimetric analysis curves of PUC1 before and after treatment with PETN and Tetryl.

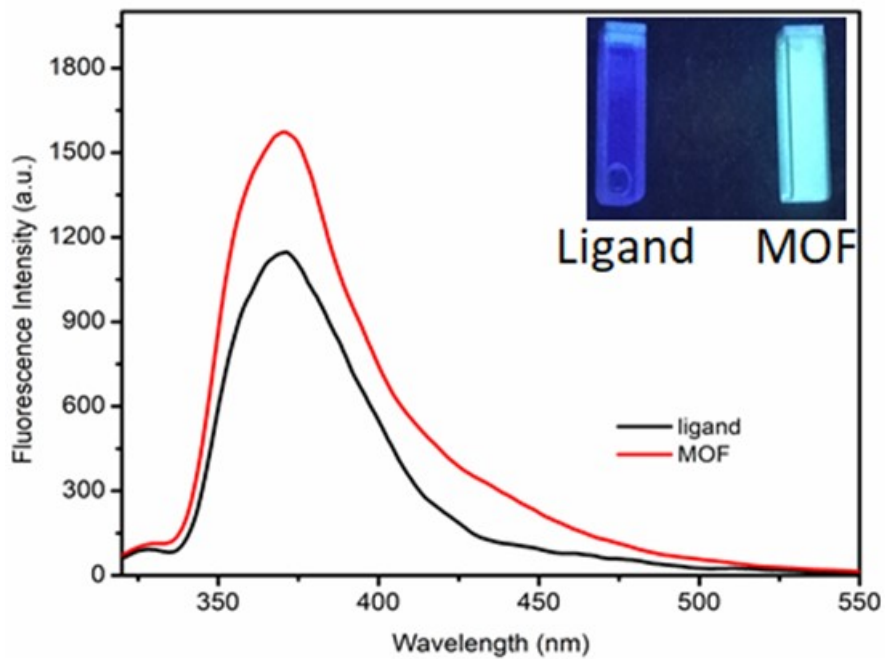


Figure S4: Fluorescence spectra of free ligand and PUC1 (inset) optical image of ligand and MOF in UV chamber.

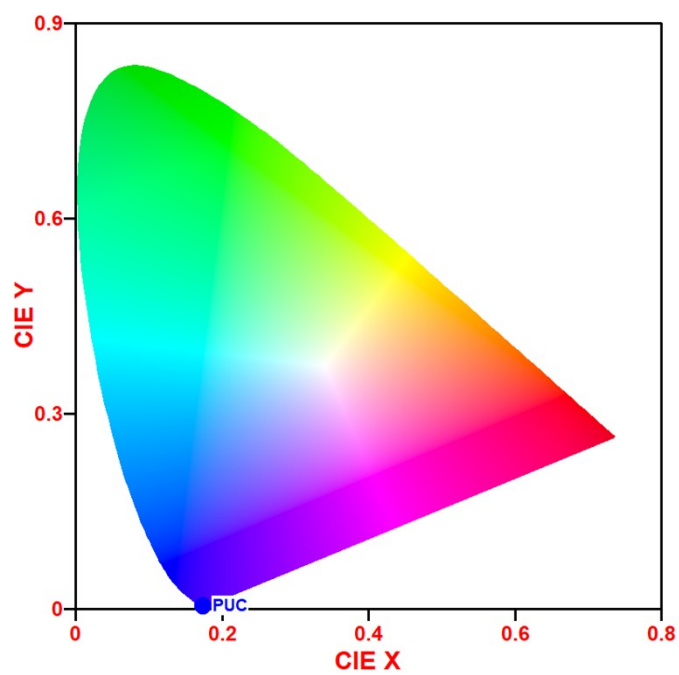
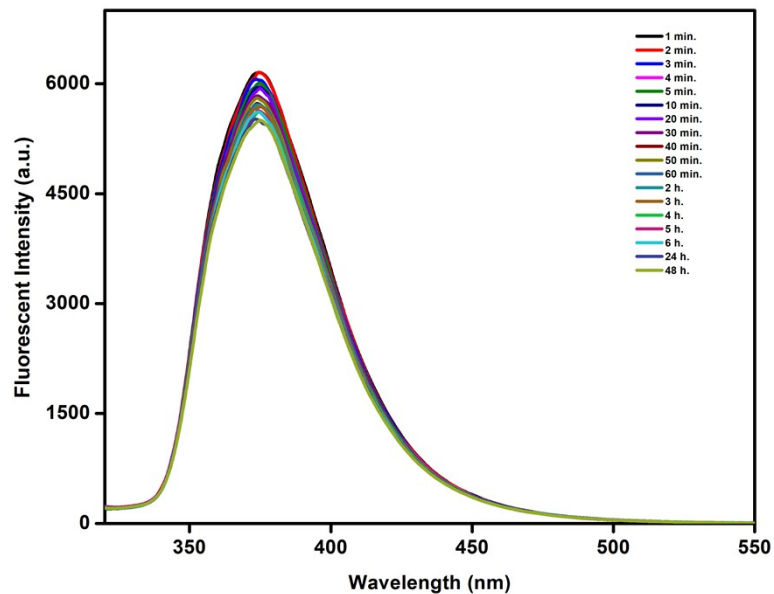


Figure S5: The CIE 1931 chromaticity diagram with CIE colour coordinates (0.170, 0.005).



FigureS6: Fluorescence spectra of PUC1 with time up to 48 hours.

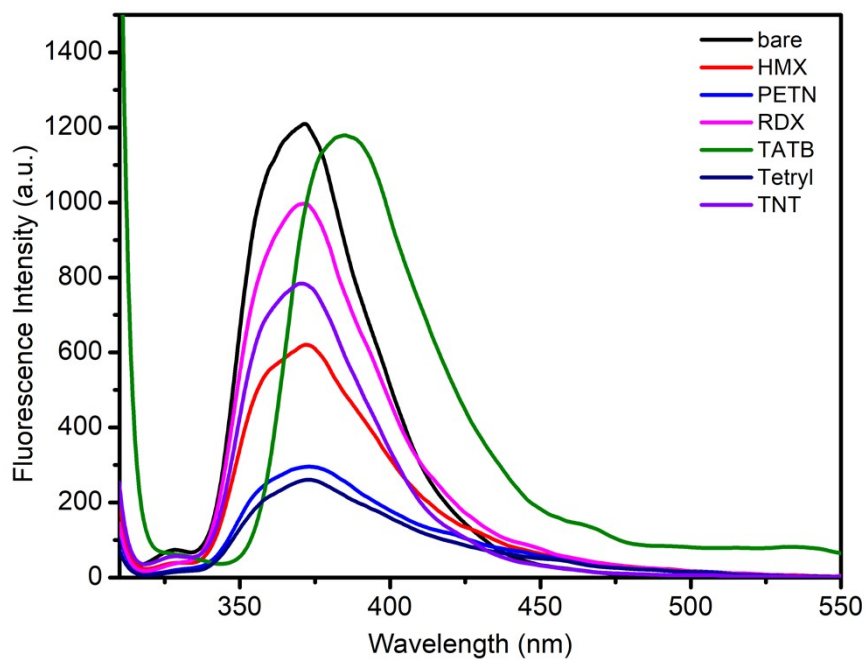


Figure S7: The fluorescence spectra of PUC1 before and after the addition of PETN, Tetryl, TATB, TNT, HMX and RDX (50 $\mu$ M).

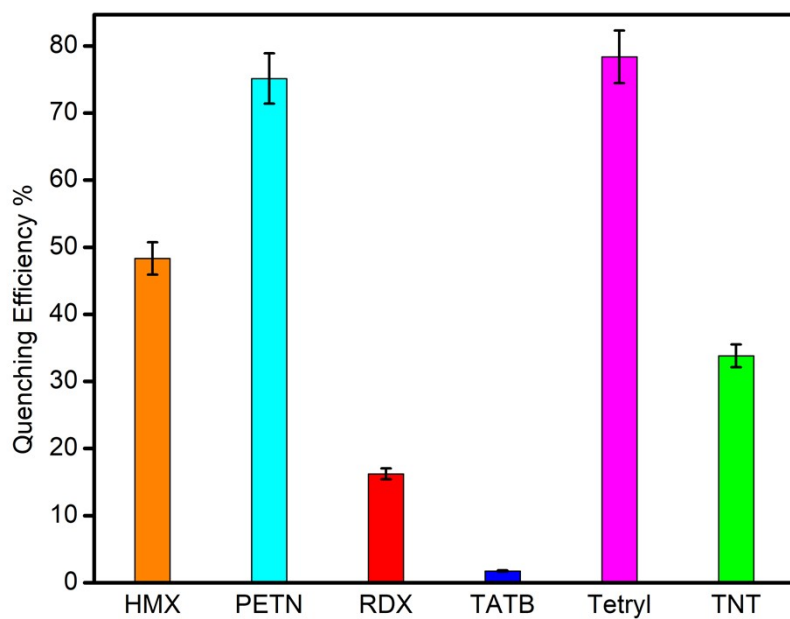


Figure S8: Quenching efficiency of different explosive compounds.

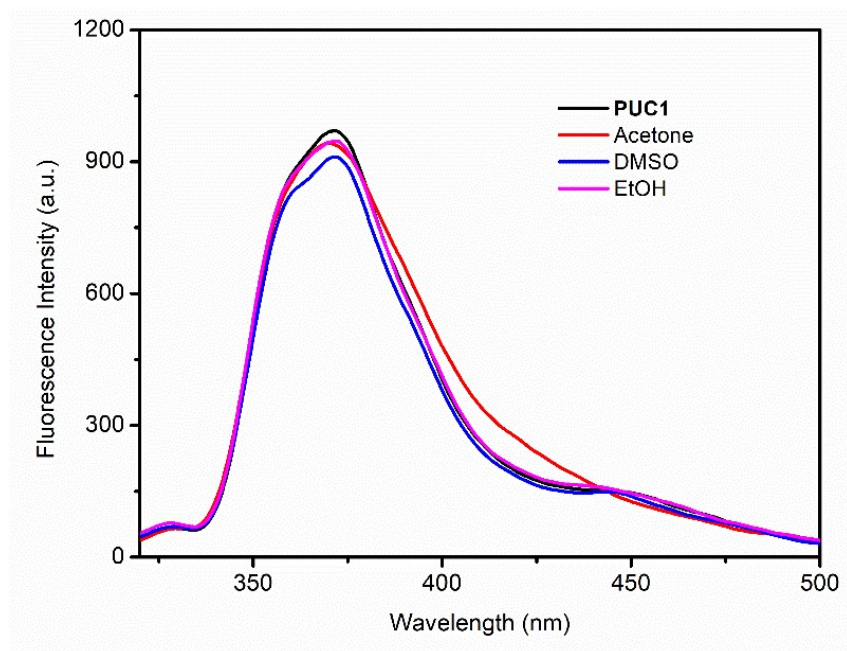


Figure S9: Fluorescence spectra of PUC1 before and after addition of different solvents.

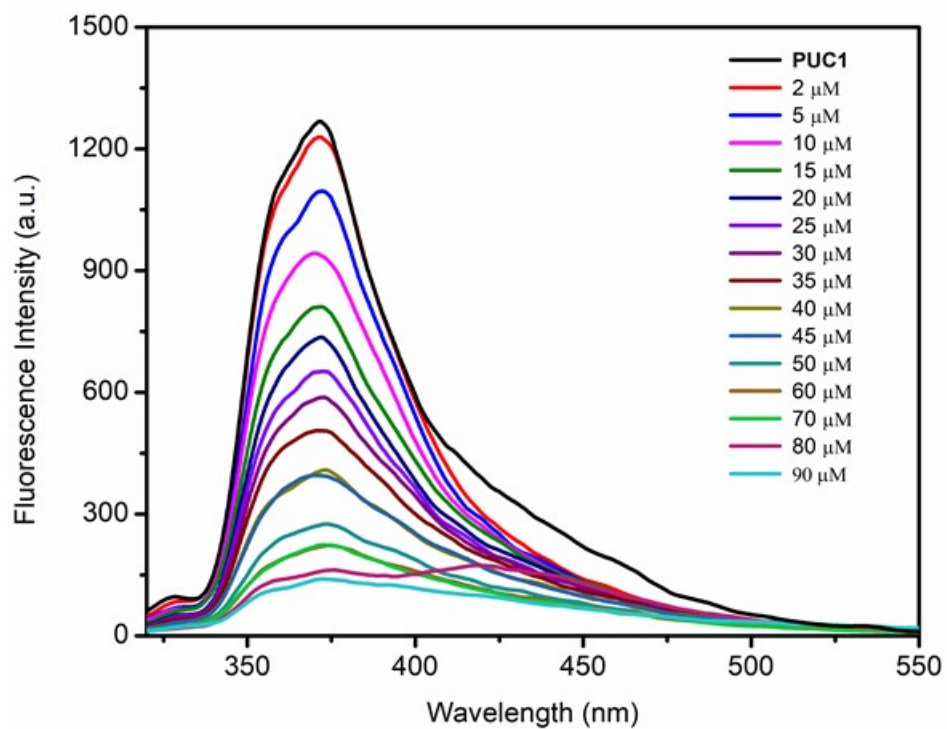


Figure S10: Fluorescence spectra of **PUC1** by gradual addition of PETN (90μM).

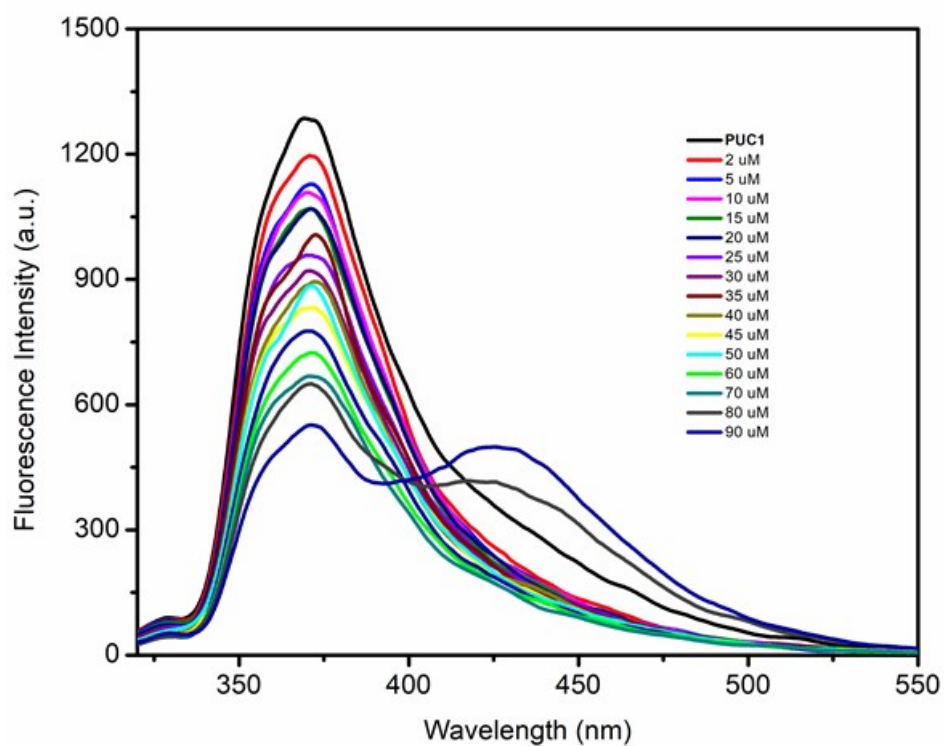


Figure S11: Fluorescence spectra of **PUC1** by gradual addition of Tetryl (90μM).



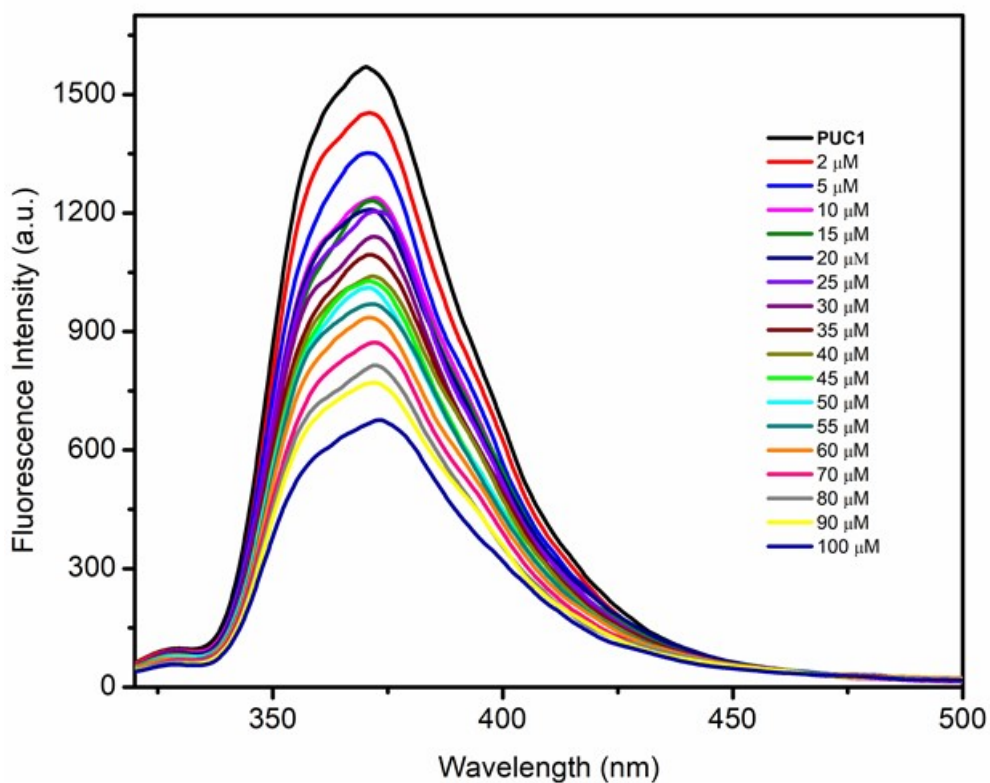


Figure S12: Fluorescence spectra of **PUC1** by gradual addition of TNT (100μM).

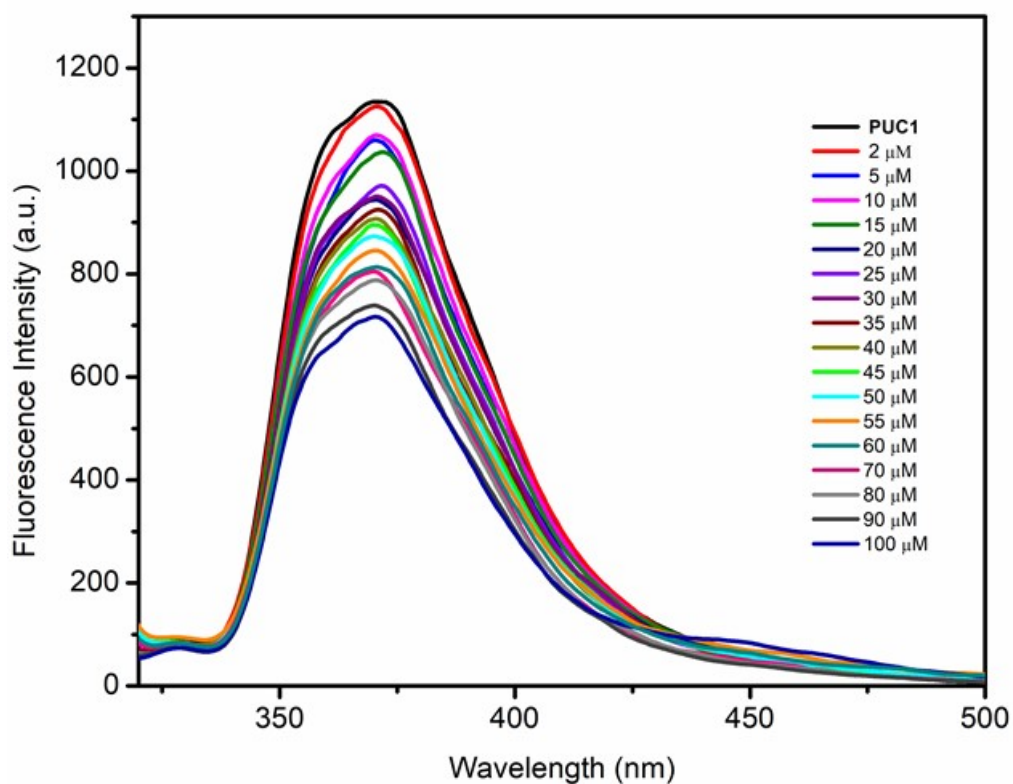


Figure S13: Fluorescence spectra of **PUC1** by gradual addition of HMX (100μM).



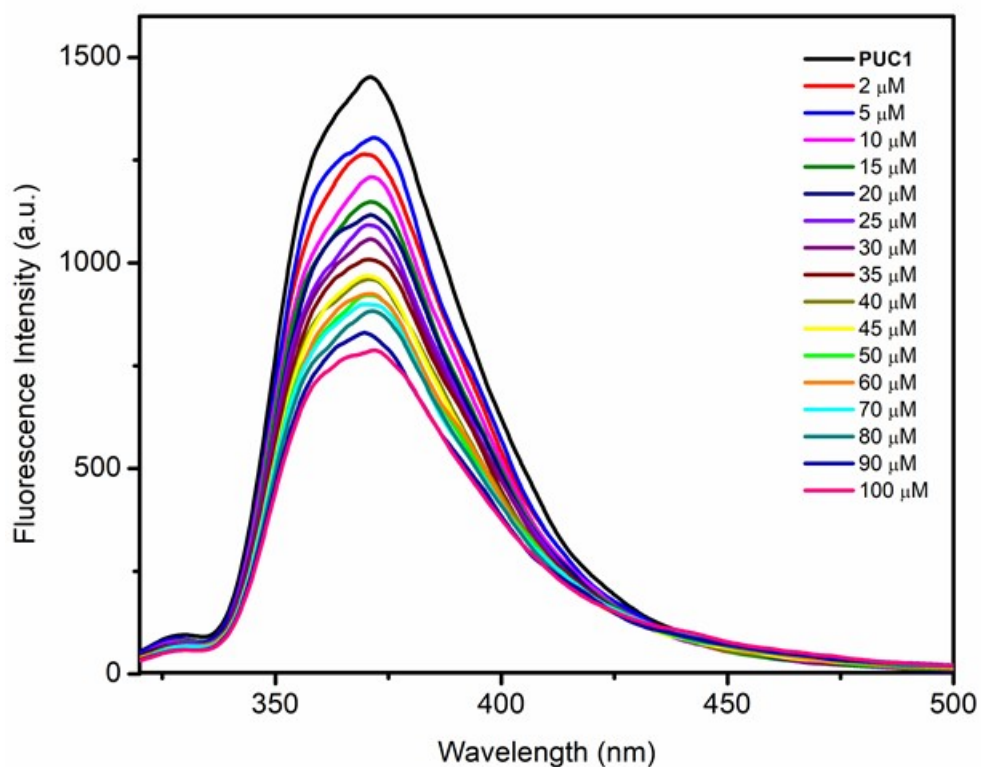


Figure S14: Fluorescence spectra of **PUC1** by gradual addition of RDX (100 $\mu$ M).

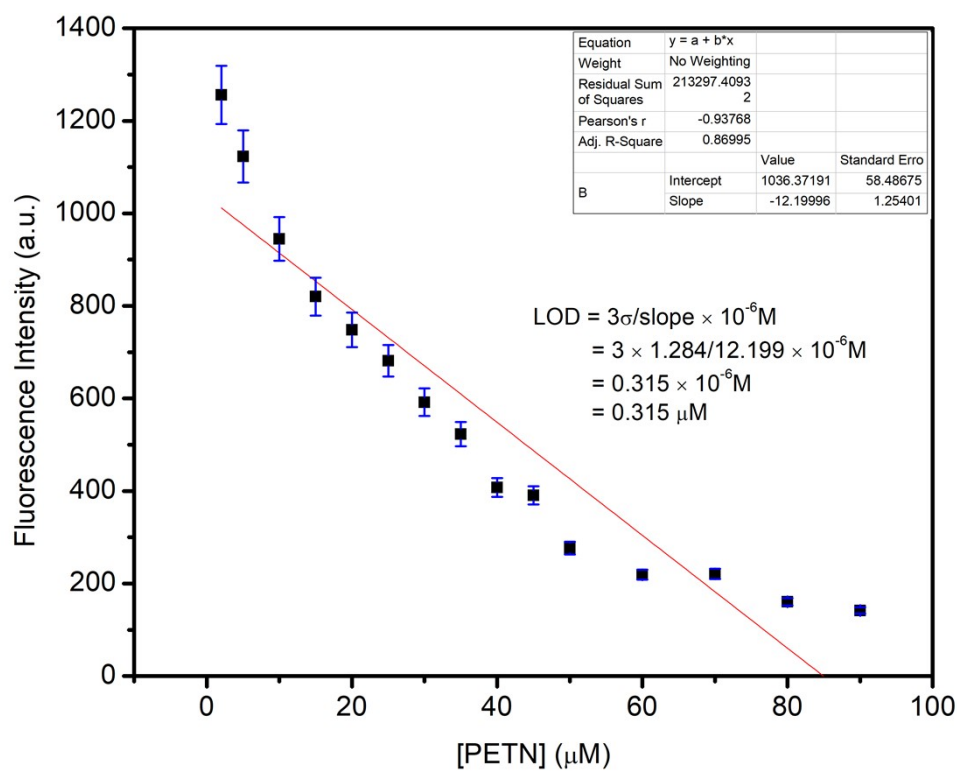


Figure S15: Estimation of limit of detection of **PUC1** for PETN.

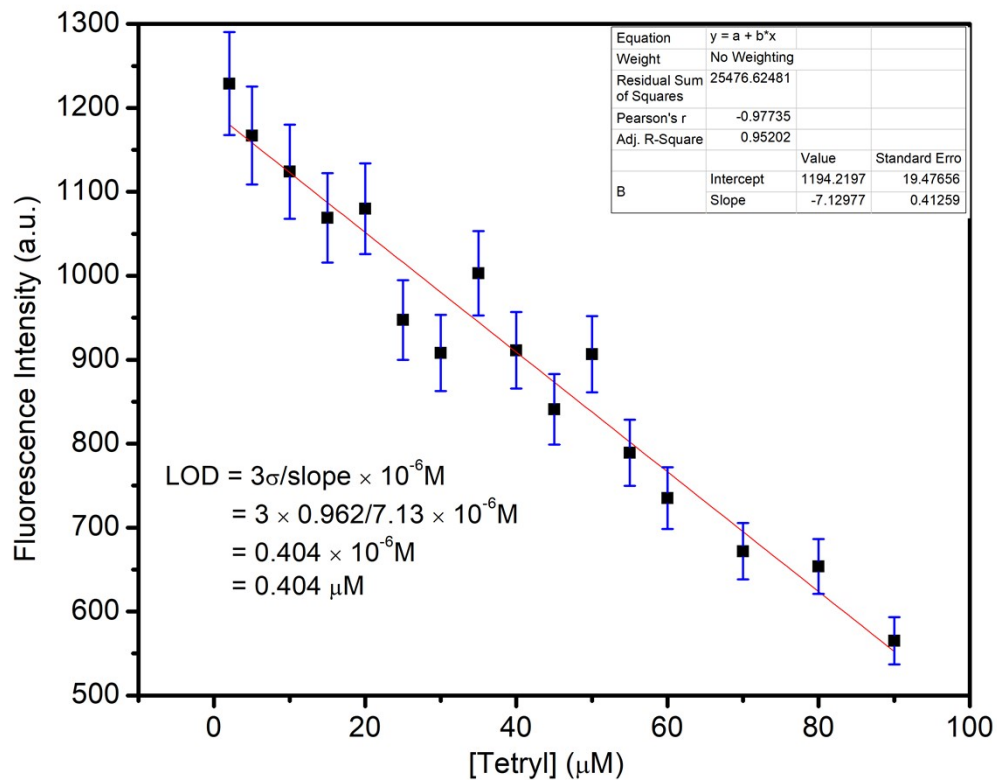


Figure S16: Estimation of limit of detection of **PUC1** for Tetryl.

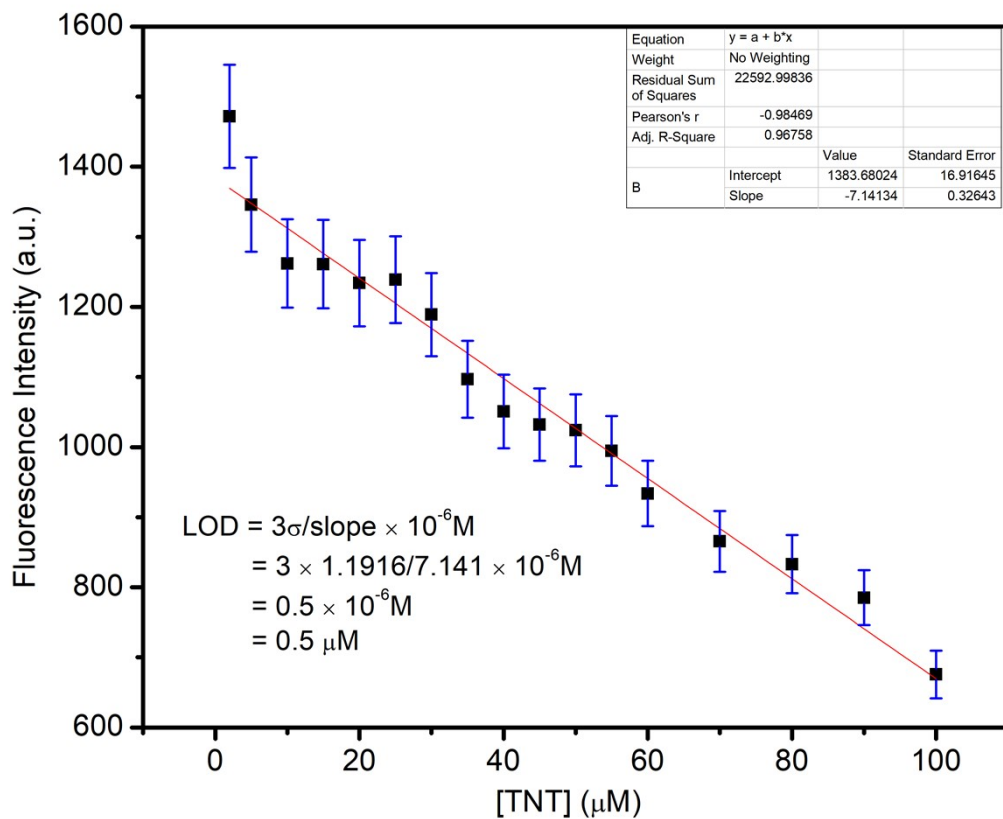


Figure S17: Estimation of limit of detection of **PUC1** for TNT.

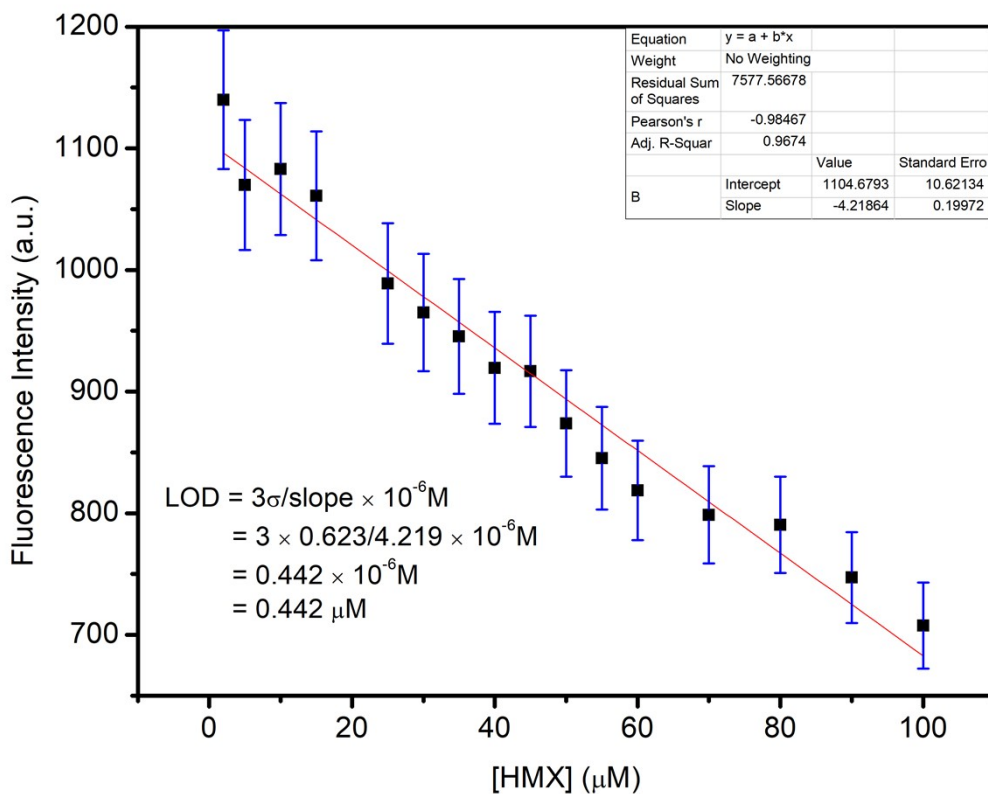


Figure S18: Estimation of limit of detection of **PUC1** for HMX.

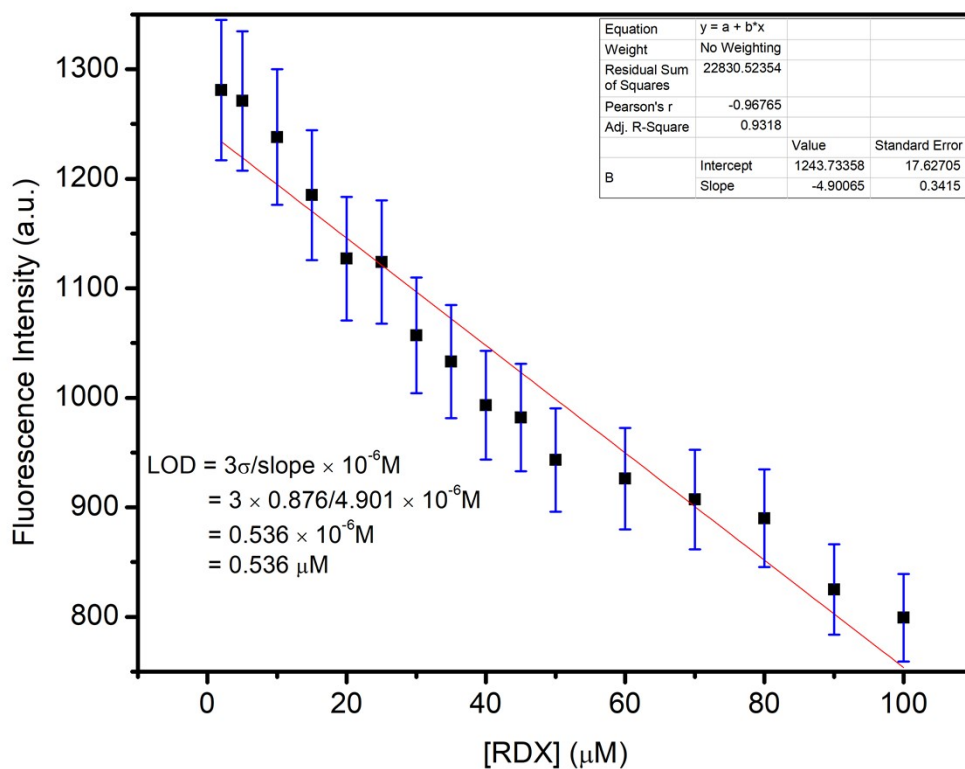


Figure S19: Estimation of limit of detection of **PUC1** for RDX.

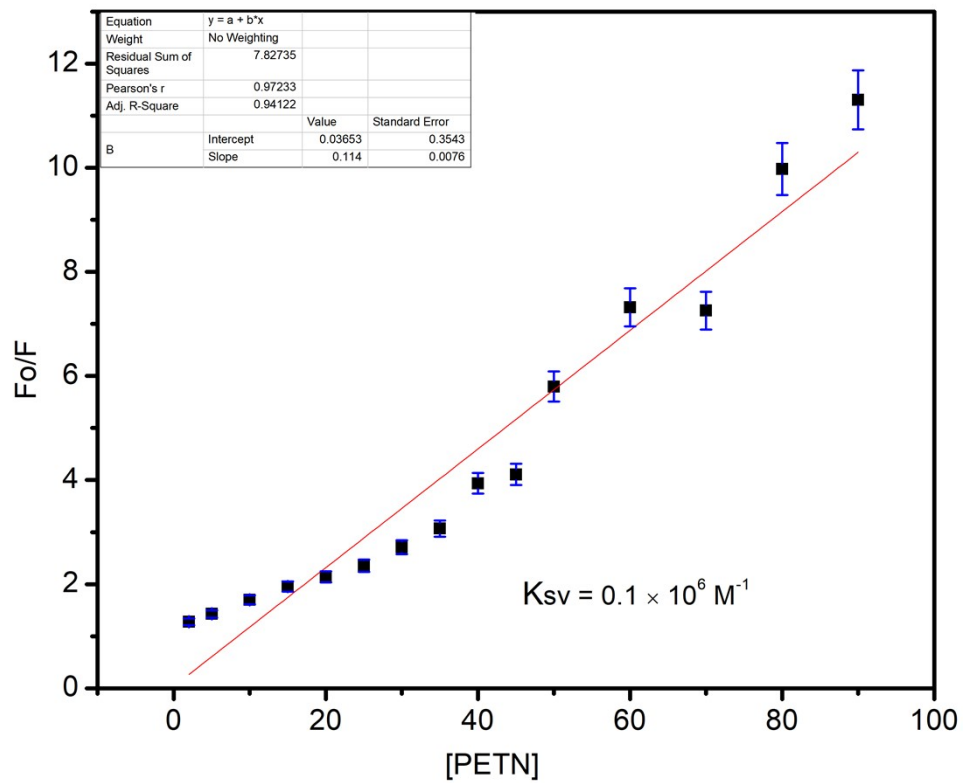


Figure S20: Stern-Volmer plots of **PUC1** by gradual addition of PETN (90 $\mu$ M).

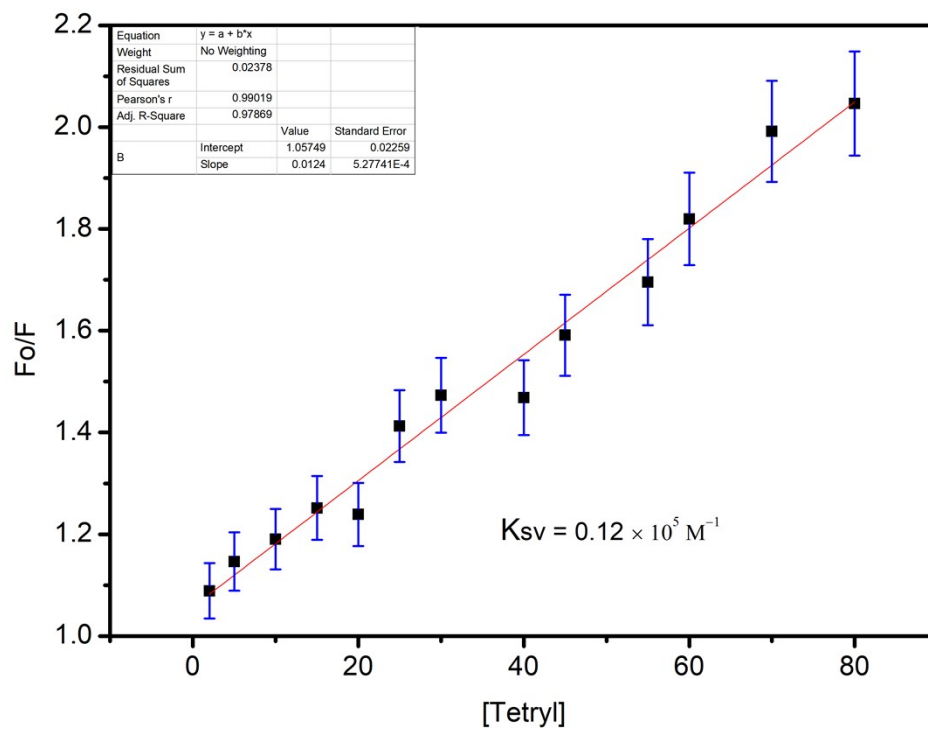


Figure S21: Stern-Volmer plots of **PUC1** by gradual addition of Tetryl (90 $\mu$ M).

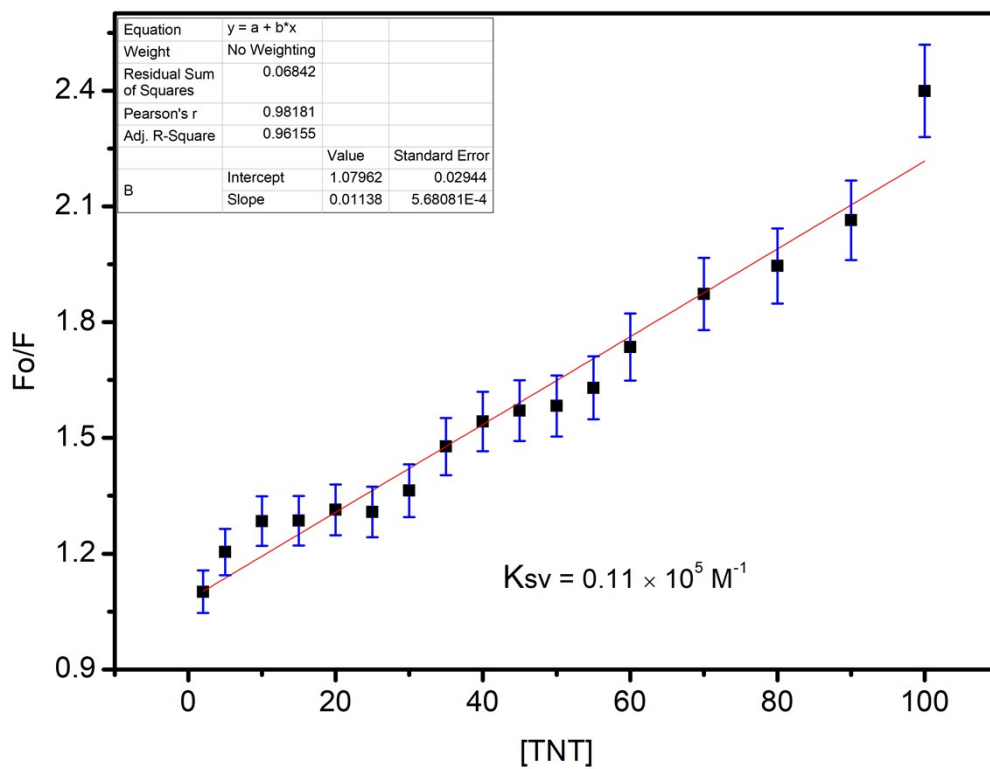


Figure S22: Stern-Volmer plots of **PUC1** by gradual addition of TNT (100 $\mu$ M).

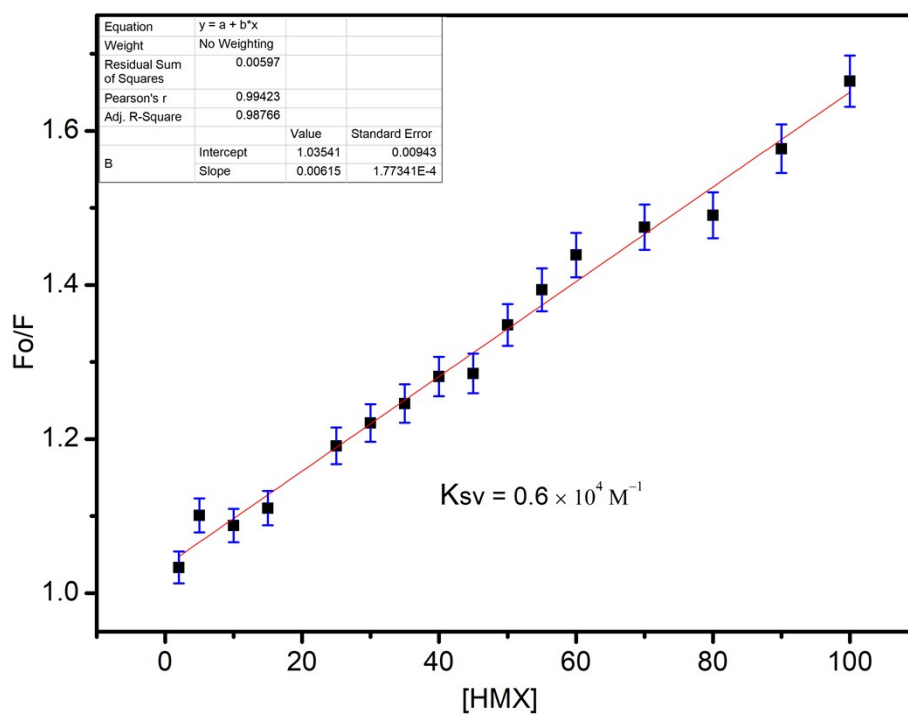


Figure S23: Stern-Volmer plots of **PUC1** by gradual addition HMX (100 $\mu$ M).

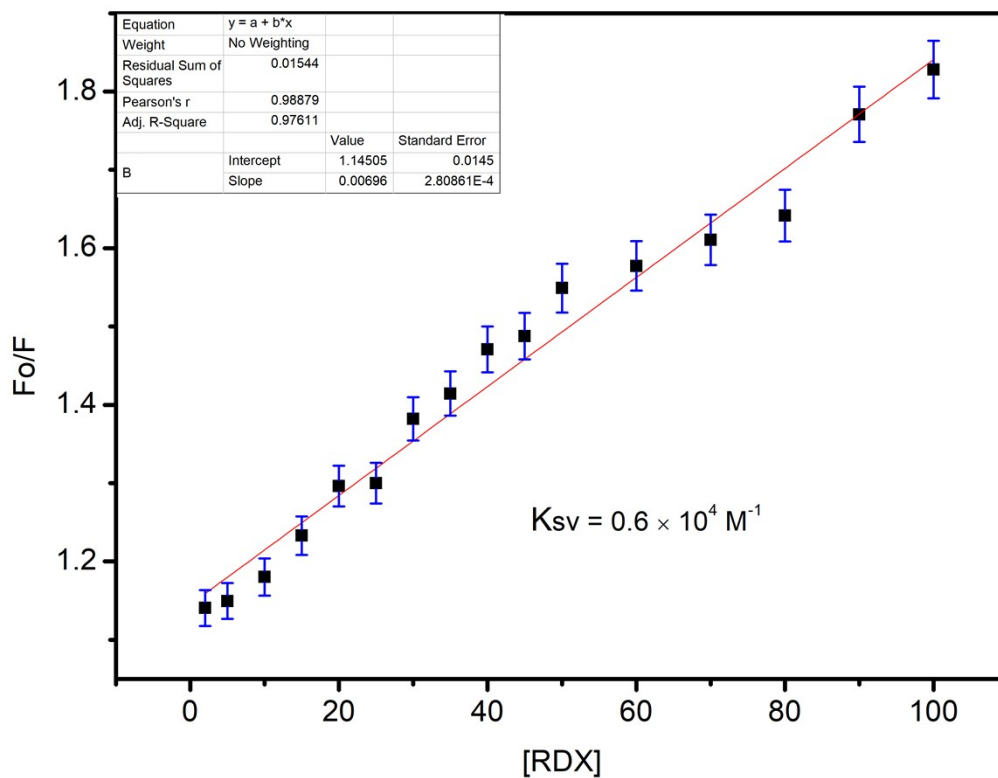


Figure S24: Stern-Volmer plots of **PUC1** by gradual addition of RDX (100 $\mu$ M).

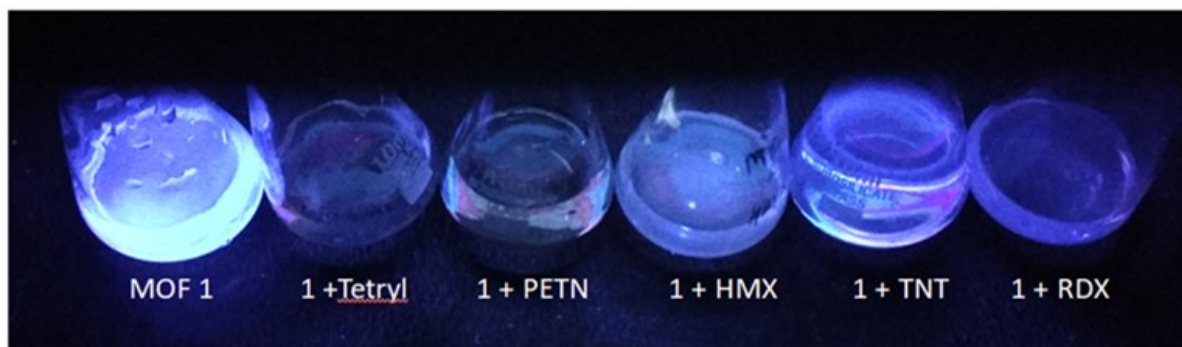


Figure S25: Optical images of PUC1 before and after the addition of analytes under UV light ( $\lambda_{\text{ext}}=365$ ).

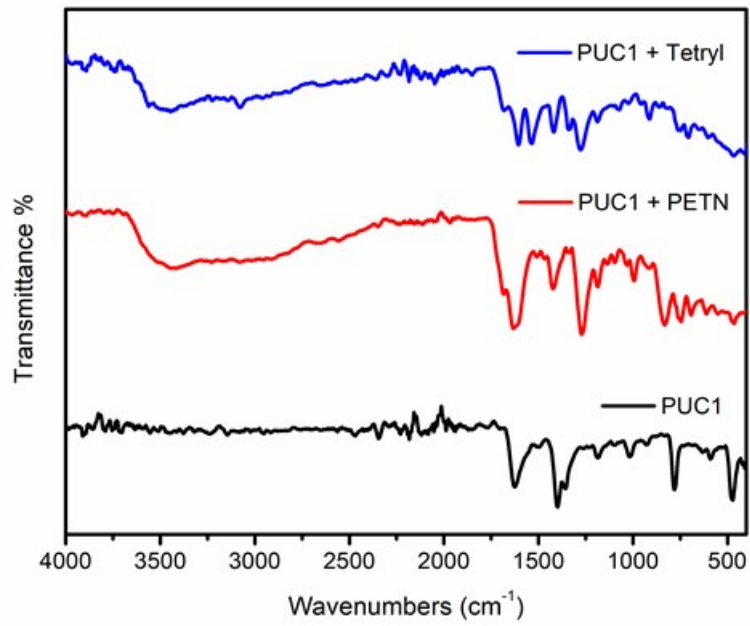


Figure S26: FTIR spectra of **PUC1** before and after addition of PETN and Tetryl.

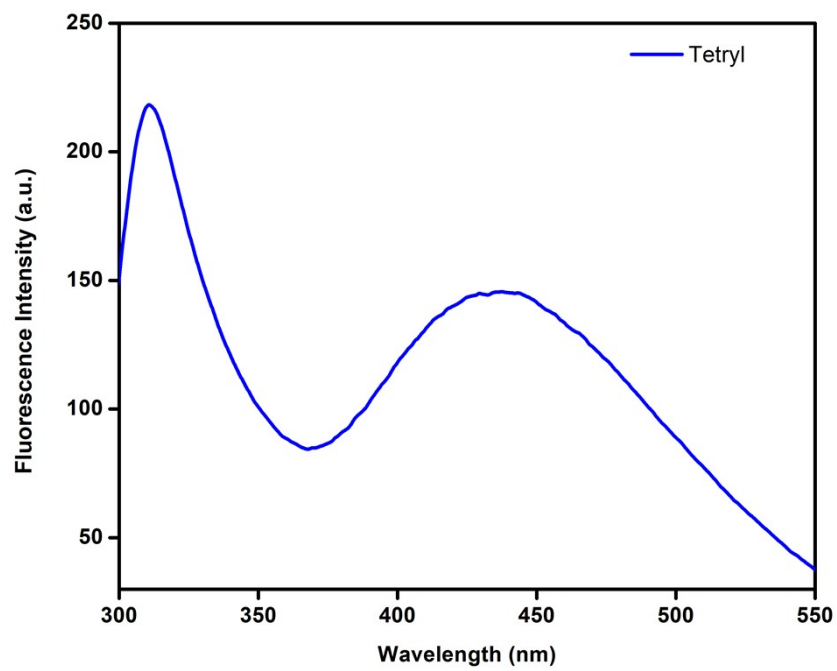


Figure S27: Fluorescence spectra of Tetryl only.



Figure S28: Tauc plots of (a) PUC1; (b) PETN; (c) Tetryl; (d) TNT; (e) RDX and (f) HMX.

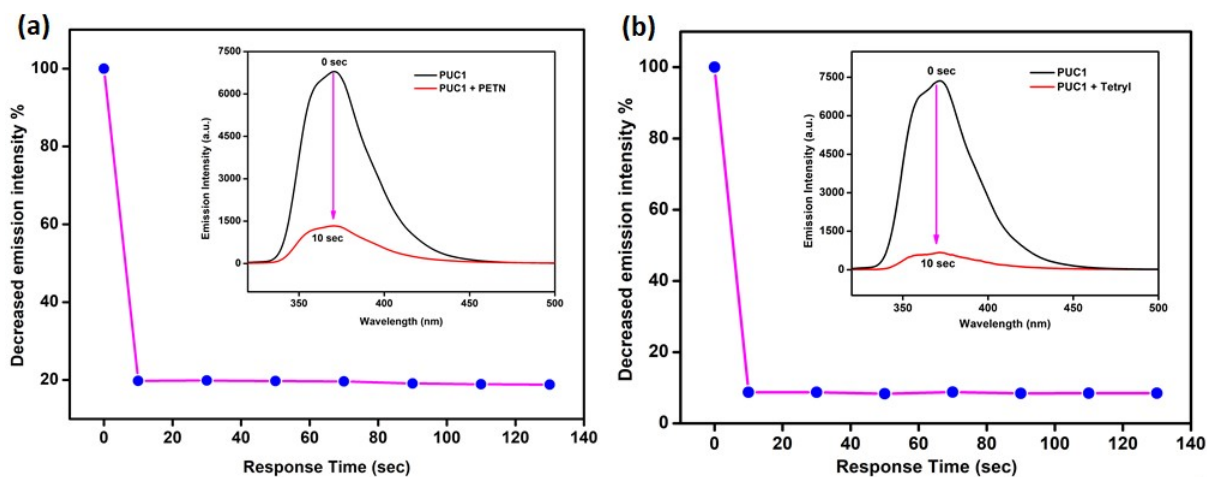
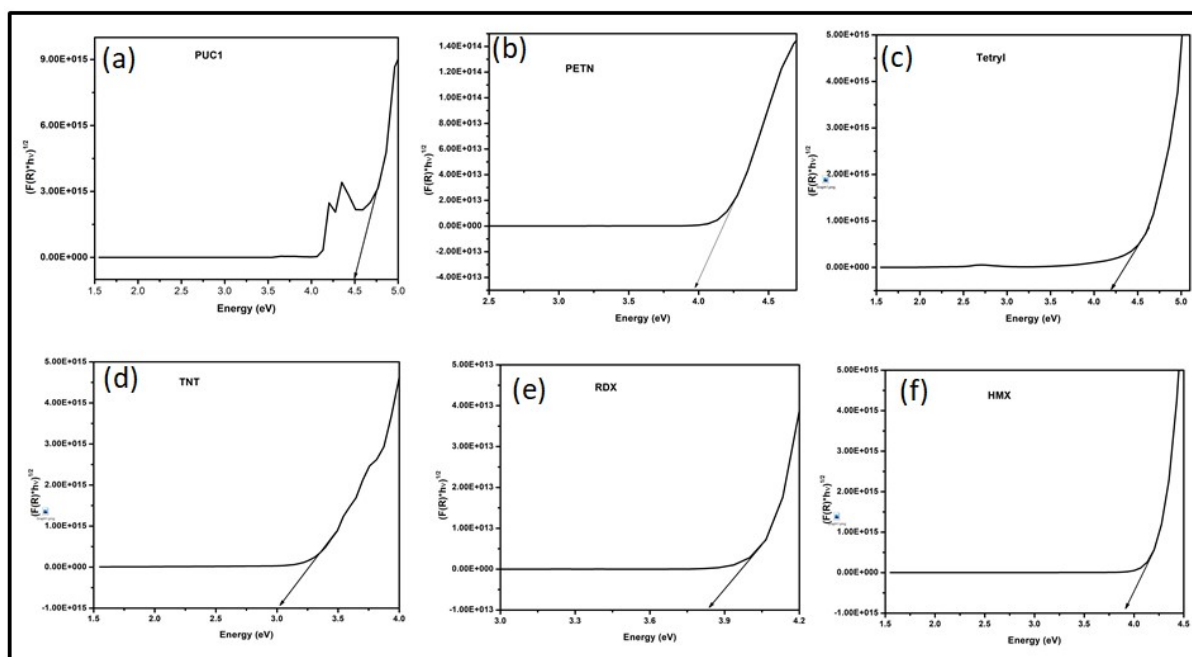


Figure S29: Plot of decrease in the emission intensity percentage at different time intervals for (a) PETN and (b) Tetryl. Inset shows the fluorescence spectra of PUC1 before (0 s) and after (10 s) the addition of analytes.

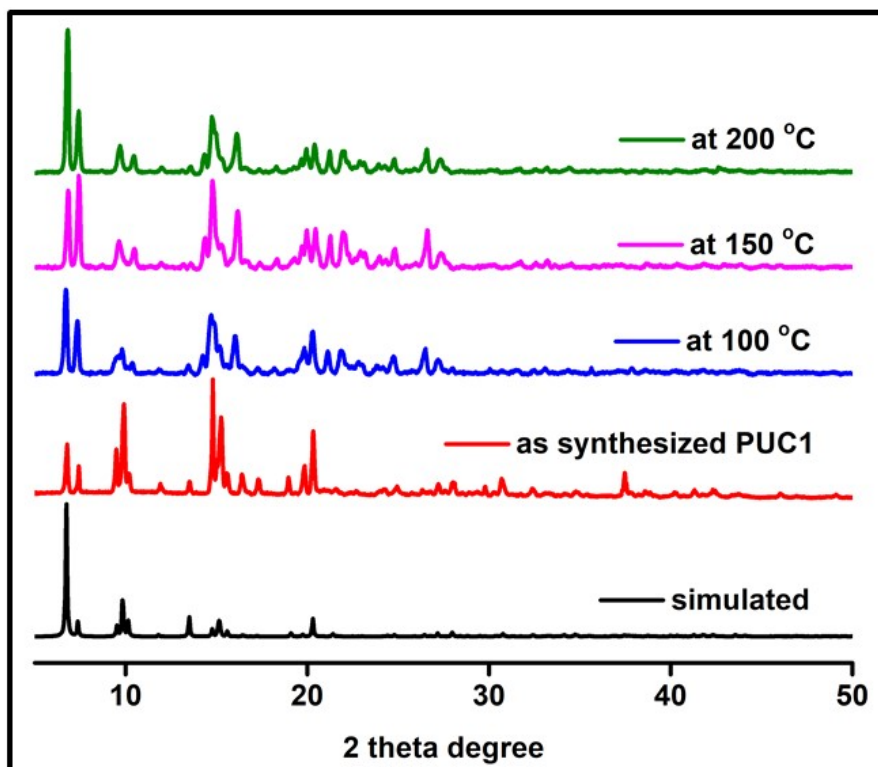


Figure S30: PXRD spectra of PUC1 at different temperatures i.e. 100, 150 and 200 °C.

Table S1: List of Crystallographic parameters for PUC1.

Identification code	<b>PUC1</b>
CCDC	2038686
Empirical formula	$C_{123}H_{52}N_8O_{32}Zn_8$
Formula weight	2676.85
Temperature/K	293(2)
Crystal system	monoclinic
Space group	C2/m
a/Å	18.1819(3)
b/Å	18.8056(4)
c/Å	23.9801(4)
$\alpha/^\circ$	90
$\beta/^\circ$	92.003(2)
$\gamma/^\circ$	90
Volume/Å <sup>3</sup>	8194.3(3)
Z	2
$\rho_{\text{calc}}/\text{cm}^3$	1.085
$\mu/\text{mm}^{-1}$	1.209
F(000)	2684.0
Crystal size/mm <sup>3</sup>	0.12 × 0.10 × 0.08
Radiation	MoK $\alpha$ ( $\lambda =$
Index ranges	-23 ≤ h ≤ 22, -16 ≤ k ≤ 24, -31 ≤ l ≤ 27
Reflections collected	37268
Independent reflections	9018 [R <sub>int</sub> =
	0.0655, R <sub>sigma</sub> = 0.0474]
Data/restraints/parameters	9018/150/514
Goodness-of-fit on F <sup>2</sup>	1.098
Final R indexes [I ≥ 2σ (I)]	R <sub>1</sub> = 0.0961, wR <sub>2</sub> = 0.2741
Final R indexes [all data]	R <sub>1</sub> = 0.1159, wR <sub>2</sub> = 0.2850

Largest diff. peak/hole / e Å<sup>-3</sup> 2.05/-2.47

Table S2: List of selected bond lengths for PUC1.

<b>Atom</b>	<b>Atom</b>	<b>Length/Å</b>
Zn3	Zn4 <sup>1</sup>	2.9602(13)
Zn3	O5 <sup>2</sup>	2.019(6)
Zn3	O5	2.019(6)
Zn3	O8 <sup>3</sup>	2.019(6)
Zn3	O8 <sup>1</sup>	2.019(6)
Zn3	N2	2.024(7)
Zn1	Zn2	2.9690(13)
Zn1	O2 <sup>4</sup>	2.039(5)
Zn1	O2 <sup>5</sup>	2.039(5)
Zn1	O3 <sup>2</sup>	2.023(6)
Zn1	O3	2.023(6)
Zn1	N4 <sup>6</sup>	2.064(8)
Zn4	O7	2.009(6)
Zn4	O7 <sup>7</sup>	2.009(5)
Zn4	O6 <sup>5</sup>	2.038(6)
Zn4	O6 <sup>8</sup>	2.038(6)
Zn4	N3	2.025(8)
Zn2	O4	2.015(5)
Zn2	O4 <sup>2</sup>	2.015(5)
Zn2	O1 <sup>4</sup>	2.050(5)
Zn2	O1 <sup>5</sup>	2.050(5)
Zn2	N1	2.022(8)

Table S3: Band Gap table of PUC1 and other analytes, calculated using tauc plot:

Analyte	Band gap (eV)
PUC1	4.5
Tetryl	4.2
PETN	3.95
HMX	3.9
RDX	3.8
TNT	3.0

Table S4: Comparison with the earlier reported methods.

Probes	Sensing analyte	Sensing Method	$K_{sv}$ value	LOD	Reference
Eu-MOF	Tetryl	Fluorescence	$1.09 \times 10^4$	0.1 – 0.5mM	1
Modified AuNPs	TNT & Tetryl	Colorimetric	-----	1.76 & 1.74pM	2
QDs	TNT	Fluorescence	-----	$\approx 1.2 \mu\text{g/mL}$	3
AuNPs composite	PETN	Surface Plasmon Resonance(SPR)	-----	200fM	4
Silica@TTF	Tetryl & TNT	Fluorescence	-----	3.5 & 26 $\mu\text{M}$	5
3-mercepto,2-butanone	Tetryl & TNT	Surface enhanced Raman scattering (SERS)	-----	17.2 & 6.81ng/ml <sup>-1</sup>	6
AuNPs-4-ATP + NED	PETN	Colorimetric	-----	0.12mg/L	7
AuNPs	PETN	Colorimetric	-----	0.169 $\mu\text{M/L}$	8
[Zn(NDA)(AMP)] (PUC1)	PETN, Tetryl	Fluorescence	$0.1 \times 10^6$ , $0.12 \times 10^5$ $\text{M}^{-1}$	0.315, 0.404 $\mu\text{M}$	Present work

## References:

- 1 N. He, M. Gao, D. Shen, H. Li, Z. Han and P. Zhao, *Forensic Sci. Int.*, 2019, **297**, 1–7.
- 2 N. Ular, A. Üzer, S. Durmazel, E. Erça and R. Apak, , DOI:10.1021/acssensors.8b00709.
- 3 W. J. Peveler, A. Roldan, N. Hollingsworth, M. J. Porter and I. P. Parkin, , DOI:10.1021/acsnano.5b06433.
- 4 M. Riskin, Y. Ben-amram, R. Tel-vered, V. Chegel, J. Almog and I. Willner, 2011, 3082–3088.
- 5 Y. Salinas, R. Martínez-Máñez, J. O. Jeppesen, L. H. Petersen, F. Sancenón, M. D. Marcos, J. Soto, C. Guillem and P. Amorós, *ACS Appl. Mater. Interfaces*, 2013, **5**, 1538–1543.
- 6 K. Milligan, N. C. Shand, D. Graham and K. Faulds, *Anal. Chem.*, 2020, **92**, 3253–3261.
- 7 A. Üzer, U. Yalçın, Z. Can, E. Erçağ and R. Apak, *Talanta*, 2017, **175**, 243–249.
- 8 Z. Taefi, F. Ghasemi and M. R. Hormozi-Nezhad, *Spectrochim. Acta - Part A Mol. Biomol. Spectrosc.*, , DOI:10.1016/j.saa.2019.117803.